PICTORIAL REVIEW

Causes and imaging features of false positives and false negatives on ^{18}F-PET/CT in oncologic imaging

Niamh M. Long · Clare S. Smith

Abstract

Background 18F-FDG is a glucose analogue that is taken up by a wide range of malignancies. 18F-FDG PET-CT is now firmly established as an accurate method for the staging and restaging of various cancers. However, 18F-FDG also accumulates in normal tissue and other non-malignant conditions, and some malignancies do not take up F18-FDG or have a low affinity for the tracer, leading to false-positive and false-negative interpretations.
Methods PET-CT allows for the correlation of two separate imaging modalities, combining both morphological and metabolic information. We should use the CT to help interpret the PET findings. In this article we will highlight specific false-negative and false-positive findings that one should be aware of when interpreting oncology scans.
Results We aim to highlight post-treatment conditions that are encountered routinely on restaging scans that can lead to false-positive interpretations. We will emphasise the importance of using the CT component to help recognise these entities to allow improved diagnostic accuracy.
Conclusion In light of the increased use of PET-CT, it is important that nuclear medicine physicians and radiologists be aware of these conditions and correlate the PET and CT components to avoid misdiagnosis, over staging of disease and unnecessary biopsies.

Keywords Oncologic imaging · PET/CT artifacts · Treatment effects · False positives · False negatives

N. M. Long · C. S. Smith (✉)
Department of Radiology, Mater Misericordiae
University Hospital,
Eccles St.,
Dublin 7, Ireland
e-mail: csmith@mater.ie

Introduction

[^{18}F] 2-fluoro-2deoxy-D-glucose (^{18}F-FDG) PET-CT imaging has become firmly established as an excellent clinical tool in the diagnosis, staging and restaging of cancer. ^{18}F-FDG (a glucose analog) is taken up by cells via glucose transporter proteins. The glucose analog then undergoes phosphorylation by hexokinase to FDG-6 phosphate. Unlike glucose, FDG-phosphate does not undergo further metabolism and so becomes trapped in the cell as the cell membrane is impermeable to FDG-6 phosphate following phosphorylation [1].

Malignant tumors have a higher metabolic rate and generally express higher numbers of specific membrane transporter proteins than normal cells. This results in increased uptake of ^{18}F-FDG by tumor cells and forms the basis of FDG-PET imaging [2]. Glucose however acts as a basic energy substrate for many tissues, and so ^{18}F-FDG activity can be seen both physiologically and in benign conditions. In addition, not all tumors take up FDG [3–5]. The challenge for the interpreting physician is to recognize these entities and avoid the many pitfalls associated with ^{18}F-FDG PET-CT imaging.

In this article we discuss false-positive and false-negative ^{18}F-FDG PET-CT findings, common and atypical physiological sites of FDG uptake, and benign pathological causes of FDG uptake. We will focus on post-treatment conditions that can result in false-positive findings. We will highlight the importance of utilizing the CT component of the study, not only for attenuation correction but also in the interpretation of the study. The CT component of ^{18}F-FDG PET-CT imaging can provide high-resolution anatomical information, which enables more accurate staging and assessment. For the purposes of this article, we refer to the

descriptive terms "false-positive" and "false-negative" findings in the context of oncology imaging.

The authors acknowledge that there are recognized causes of FDG uptake that are not related to malignancy; however in this paper we refer to false-positive findings as FDG uptake that is not tumor related.

Patient preparation

Tumor uptake of FDG is reduced in the presence of raised serum glucose as glucose competes with FDG for uptake by the membrane transporter proteins. In order to prevent false-negative results, it is necessary for the patient to fast for at least 4–6 h prior to the procedure [6]. Induction of a euglycamic hypoinsulinaemic state also serves to reduce the uptake of glucose by the myocardium and skeletal muscle. In the fasting state, the decreased availability of glucose results in predominant metabolism of fatty acids by the myocardium. This reduces the intensity of myocardial uptake and prevents masking of metastatic disease within the mediastinum [6].

The radiotracer is administered intravenously (dose dependent on both the count rate capability of the system used and the patient's weight), and the patient is left resting in a comfortable position during the uptake phase (60–90 min). Patient discomfort and anxiety can result in increased uptake in skeletal muscles of the neck and paravertebral regions. Muscular contraction immediately prior to or following injection can result in increased FDG activity in major muscle groups [6].

Patients are placed in a warm, quiet room with little stimulation, as speech during the uptake phase is associated with increased FDG uptake in the laryngeal muscles [7].

At our institution we perform the CT component with arms up except for head and neck studies where the arms are placed down by the side. This minimizes artifacts on CT. Depending on the type of cancer, oral contrast to label the bowel and intravenous contrast may also be given. The CT is performed with a full dose similar to a diagnostic CT, and lungs are analyzed following reconstruction with a lung algorithm. The PET scan is performed with 3–4 min per bed position; however the

Fig. 1 ^{18}F-FDG PET-CT performed in a 65-year-old male with colorectal cancer. On the coronal PET images, a focus of increased FDG uptake is seen at the right lung base (black arrow). Contrast CT does not show any pulmonary nodules but does demonstrate a liver metastasis in the superior aspect of the right lobe of the liver (yellow arrow)
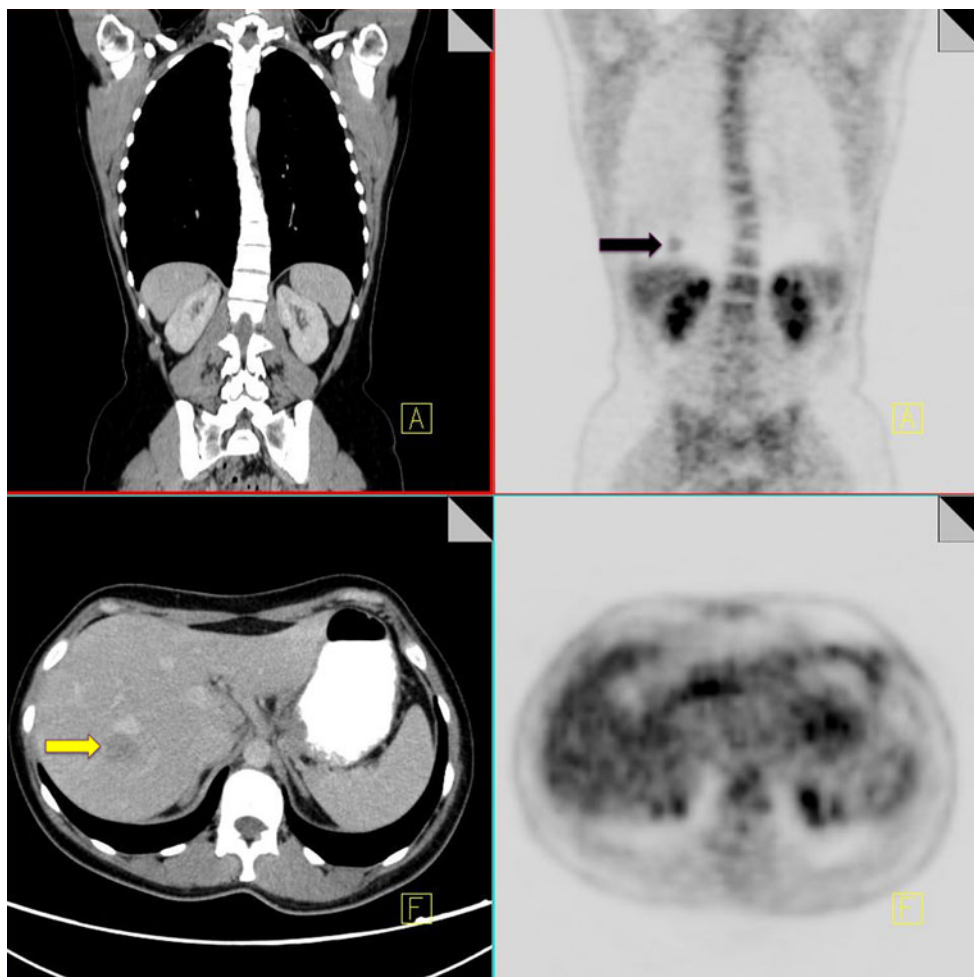
time per bed position will vary in different centers depending on both the dose of FDG administered and the specifications of the camera used for image acquisition. It is beyond the scope of this article to provide detailed procedure guidelines for ^{18}F-FDG PET-CT imaging, and for this purpose we refer the reader to a comprehensive paper by Boellaard et al. [8].

Technical causes of false positives

Misregistration artifact

The evaluation of pulmonary nodules provides a unique challenge for combined PET-CT scanning due to differences in breathing patterns between CT and PET acquisition

Fig. 2 ^{18}F-FDG PET-CT performed in a 28-year-old male with an osteosarcoma of the femur. A focus of increased FDG uptake (yellow arrow) is identified in the left lower lobe with no CT correlate (**a**). A 3-month follow-up CT thorax again does not demonstrate any pulmonary nodules confirming that the uptake seen originally on the PET-CT was due to injected clot (**b**)
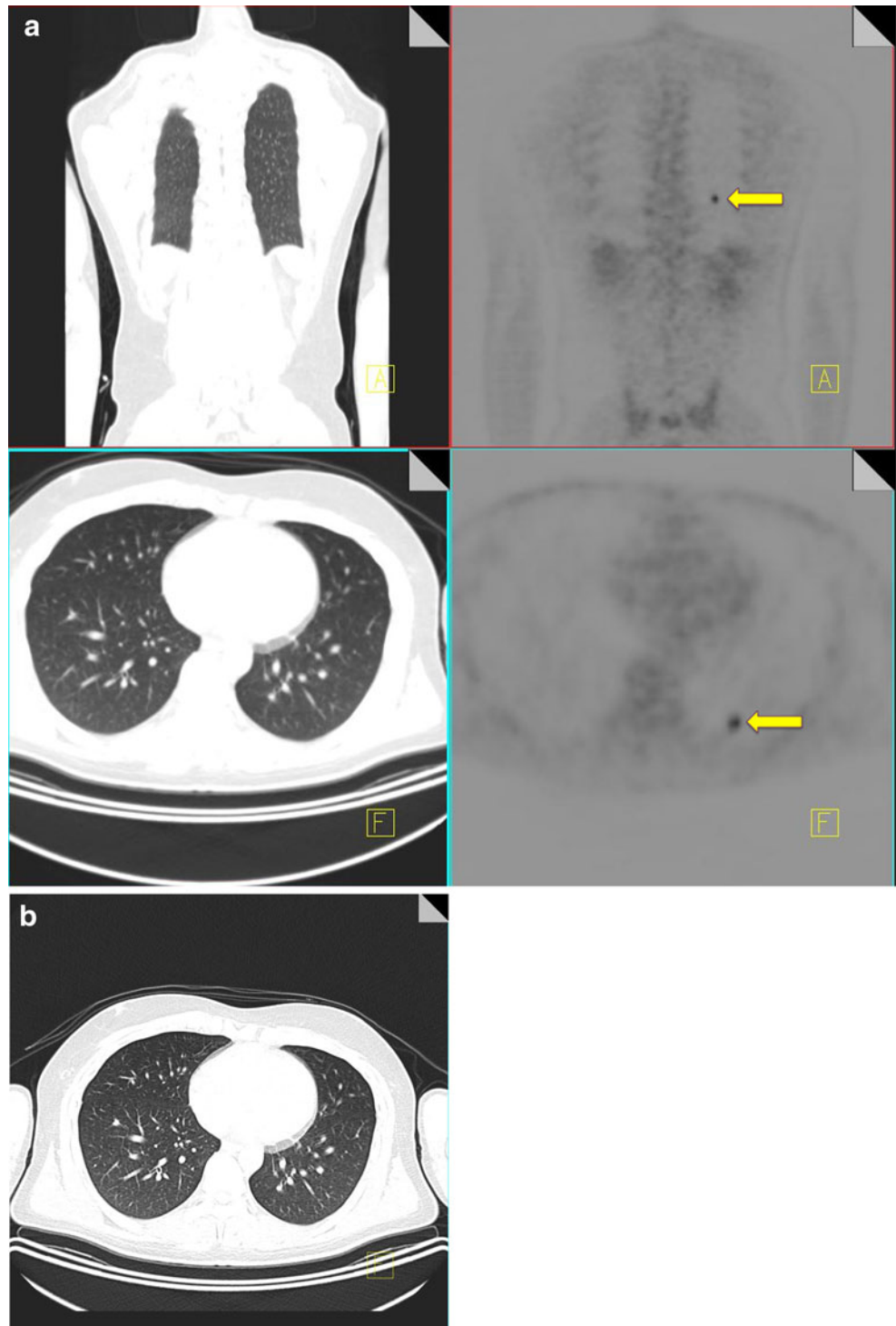
periods. CT imaging of the thorax is classically performed during a breath-hold; however PET images are acquired during tidal breathing, and this can contribute significantly to misregistration of pulmonary nodules on fused PET-CT images. Misregistration is particularly evident at the lung bases, which can lead to difficulty differentiating pulmonary nodules from focal liver lesions (Fig. 1) [9].

Acquiring CT imaging of the thorax during quiet respiration can help to minimize misregistration artifacts. It is also important to correlate your PET and CT findings by scrolling up and down to make sure that lesions match.

Injected clot A further diagnostic pitfall in staging of intrathoracic disease can be caused by injected clot. Injection of radioactive clot following blood withdrawal into the syringe at the time of radiotracer administration can result in pulmonary hotspots [10]. The absence of a CT correlate for a pulmonary hotspot should raise the possibility of injected clot; however this is a diagnosis of exclusion, and it is important to carefully evaluate the adjacent slices

to ensure the increased radiotracer activity does not relate to misregistration of a pulmonary nodule or hilar lymph node. The area of abnormal radiotracer uptake should also be closely evaluated on subsequent restaging CT to ensure there has been no interval development of an anatomical abnormality in the region of previously diagnosed injected clot (Fig. 2) [11].

Injection artifact

Leakage of radiotracer into the subcutaneous tissues at the injection site or tissued injection can result in subcutaneous tracking of FDG along lymphatic channels in the arm. This can result in spurious uptake in axillary nodes distal to the injection site [12]. Careful attention must be paid to the technical aspects of the study to ensure accurate staging. Injection at the side contralateral to the site of disease is advised where feasible to allow differentiation between artifactual and metastatic uptake, particularly in breast cancer patients. The side of injection should also be clearly documented during administration of radiotracer, and this


Fig. 3 ^{18}F-FDG PET-CT performed in a 56-year-old woman with colorectal cancer. Some low grade FDG uptake is identified in non-enlarged right axillary nodes (yellow arrow) consistent with injection artifact
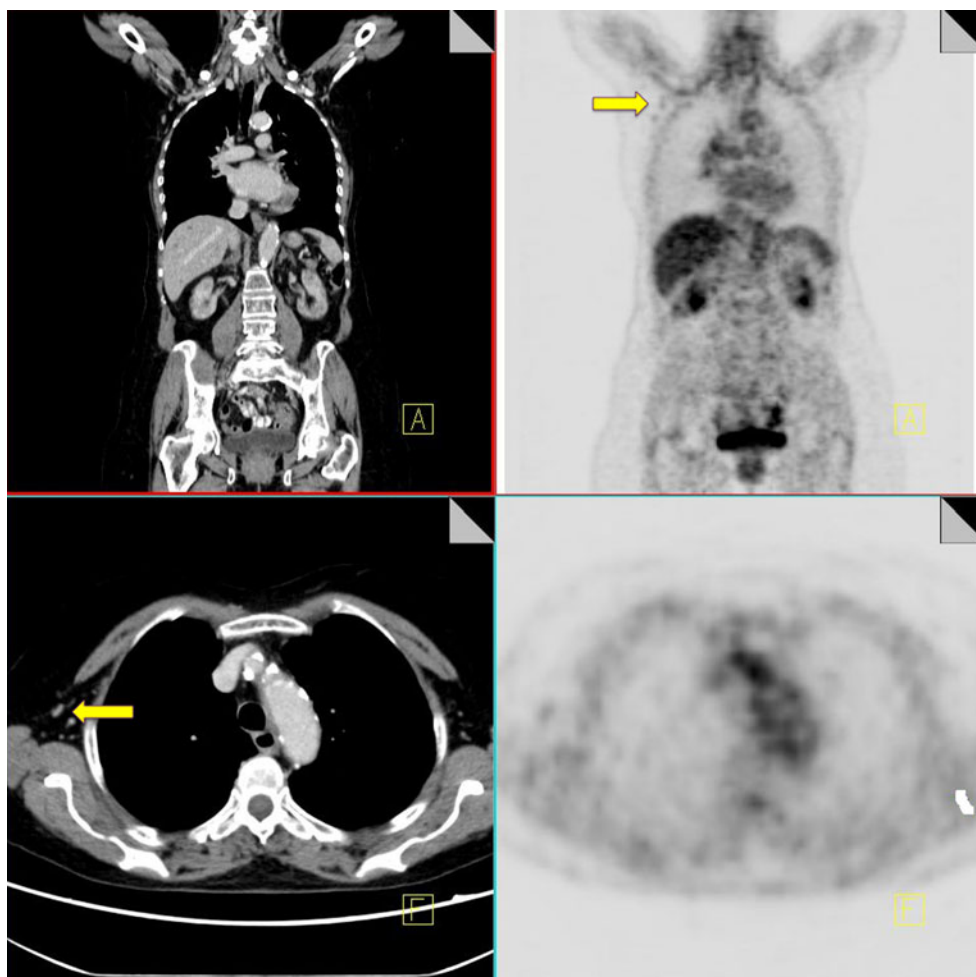
Fig. 4 ^{18}F-FDG PET-CT surveillance scan performed in a 36-year-old male with a history of seminoma. Symmetrical uptake is noted in the neck, supraclavicular fossa and paravertebral regions consistent with typical appearance of brown fat activity (black arrow). Brown fat uptake is also seen in the left supradiaphragmatic region and left paraoesophageal region (yellow arrow) (**a**). ^{18}F-FDG PET-CT performed in a 48-year-old male with a history of colorectal cancer. Increased FDG uptake is noted within brown fat associated with lipomatous hypertrophy of the intra-atrial septum (**b**)
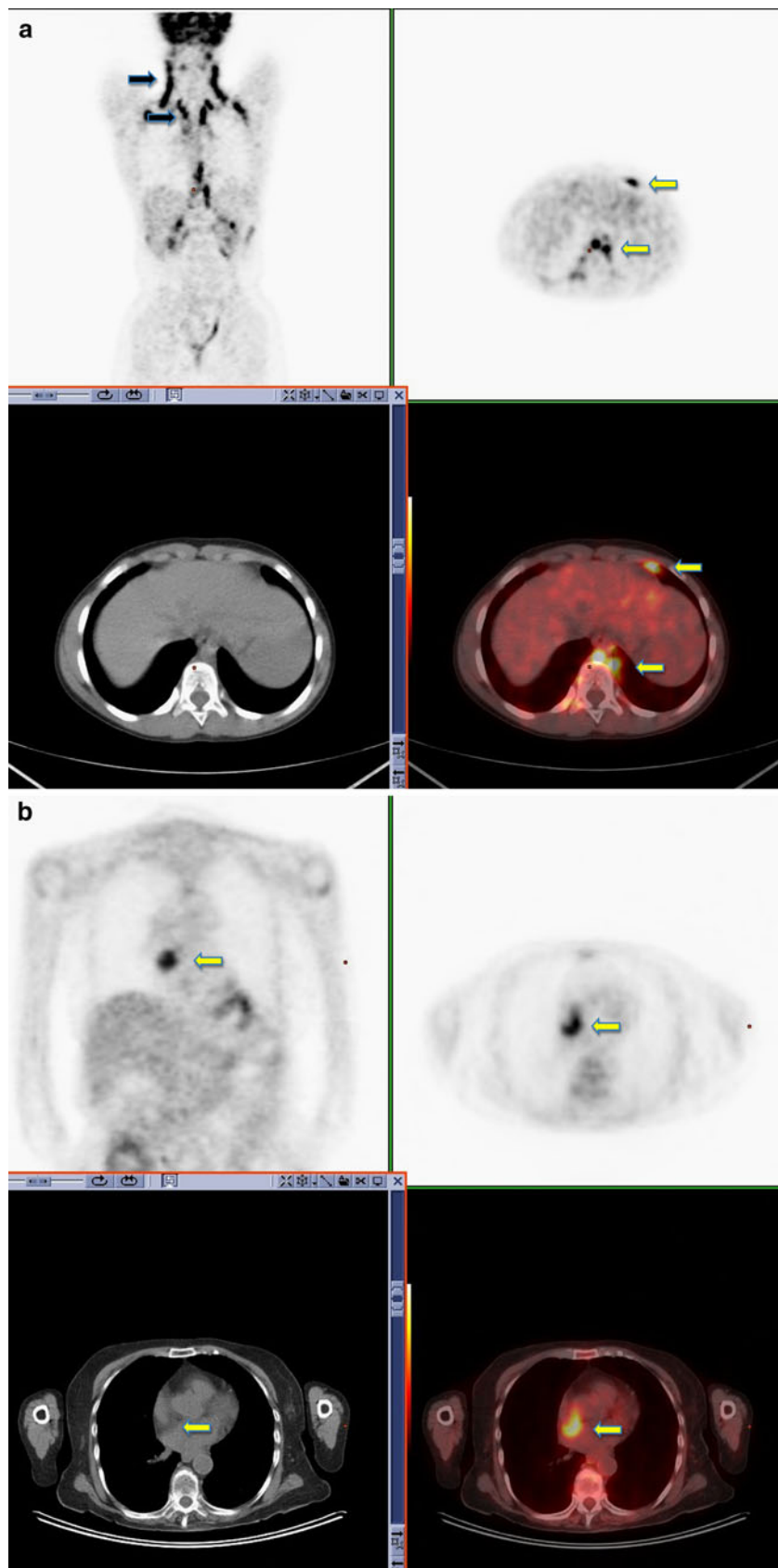
Fig. 5 ^{18}F-FDG PET-CT performed in a 42-year-old pre-menopausal female with breast cancer. She was scanned during menstruation. FDG uptake is noted within metastatic right axillary nodes (black arrow). Increased FDG uptake is also noted within the endome-trial canal of the uterus (yellow arrow), which is thickened on CT, consistent with active menstruation (**a**). ^{18}F-FDG PET-CT per-formed in the same 42-year-old woman at a different stage in her menstrual cycle showing reso-lution of the previously identi-fied uterine uptake (yellow arrow) (**b**)
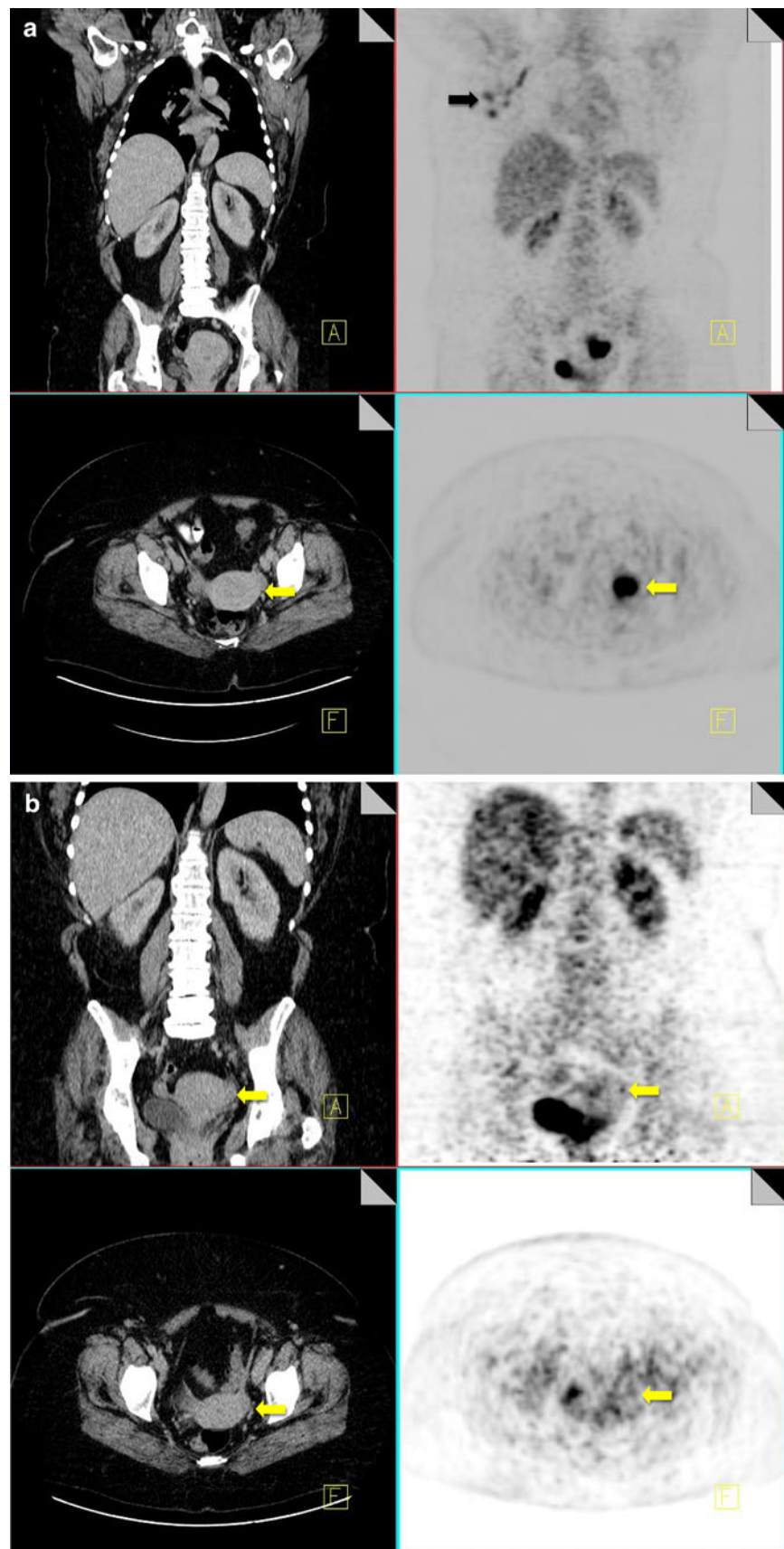
information should be available to the reader in order to ensure pathological FDG uptake is not spuriously attributed to injection artifact (Fig. 3).

Imaging of metallic implants The use of CT for attenuation correction negates the need for traditional transmission attenuation correction, reducing scanning time. There are however technical factors relating to the use of CT imaging for attenuation correction, which lead to artefacts when imaging metal [9]. The presence of metal implants in the body produces streak artifact on CT imaging and degrades image quality. When CT images are used for attenuation correction, the presence of metal results in over attenuation of PET activity in this region and can result in artifactual 'hot spots.' Metal prostheses, dental fillings, indwelling ports and breast expanders and sometimes contrast media are common causes of streak artifact secondary to high photon absorption and can cause attenuation correction artifacts [9]. In order to avoid false positives, particularly when imaging metallic implants careful attenuation should be paid to the nonattenuation corrected images, which do not produce this artifact.

Sites of physiological FDG uptake

Physiological uptake in a number of organs is readily recognized and rarely confused with malignancy. These include cerebral tissue, the urinary system, liver and spleen. Approximately 20% of administered activity is renally excreted in the 2 h post-injection resulting in intense radiotracer activity in the renal collecting systems, ureters and bladder [13]. In order to minimize the intensity of renal activity, patients are advised to void prior to imaging. Moderate physiological FDG uptake is noted in the liver, spleen, GI tract and salivary glands. Uptake in the cecum and right colon tends to be higher than in the remainder of the colon due to the presence of glucose-avid lymphocytes [14].

Other sites of physiological FDG activity can be confused with malignancy. Examples include activity within brown fat, adrenal activity, uterus and ovaries.

Brown fat FDG uptake in hyper-metabolic brown adipose tissue is well recognized as a potential source of false positive in ^{18}F-FDG PET-CT imaging. The incidence of

Fig. 6 ^{18}F-FDG PET-CT performed in a 50-year-old woman with inflammatory breast cancer. Diffuse increased FDG uptake is noted within the right breast (yellow arrow) and in a right axillary node (black arrow), consistent with malignancy (**a**). Increased symmetrical uptake is also noted within both adrenal glands with no abnormal correlate on CT (yellow arrow) (**b**). Post-chemotherapy PET-CT performed 5 months later demonstrates resolution of the activity within the breast, increased uptake in the bone marrow consistent with post treatment effect (black arrow) and persistent increased uptake in the adrenal glands (yellow arrow), confirming benign physiological activity (**c**)
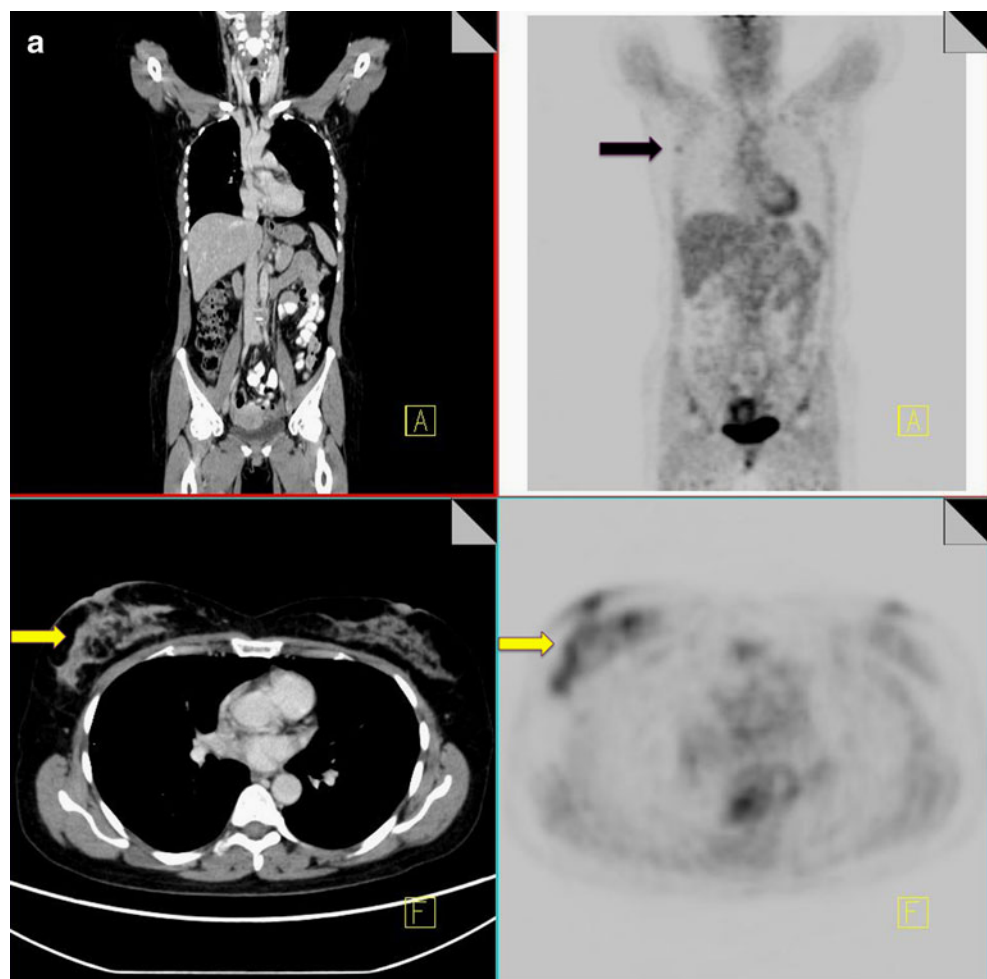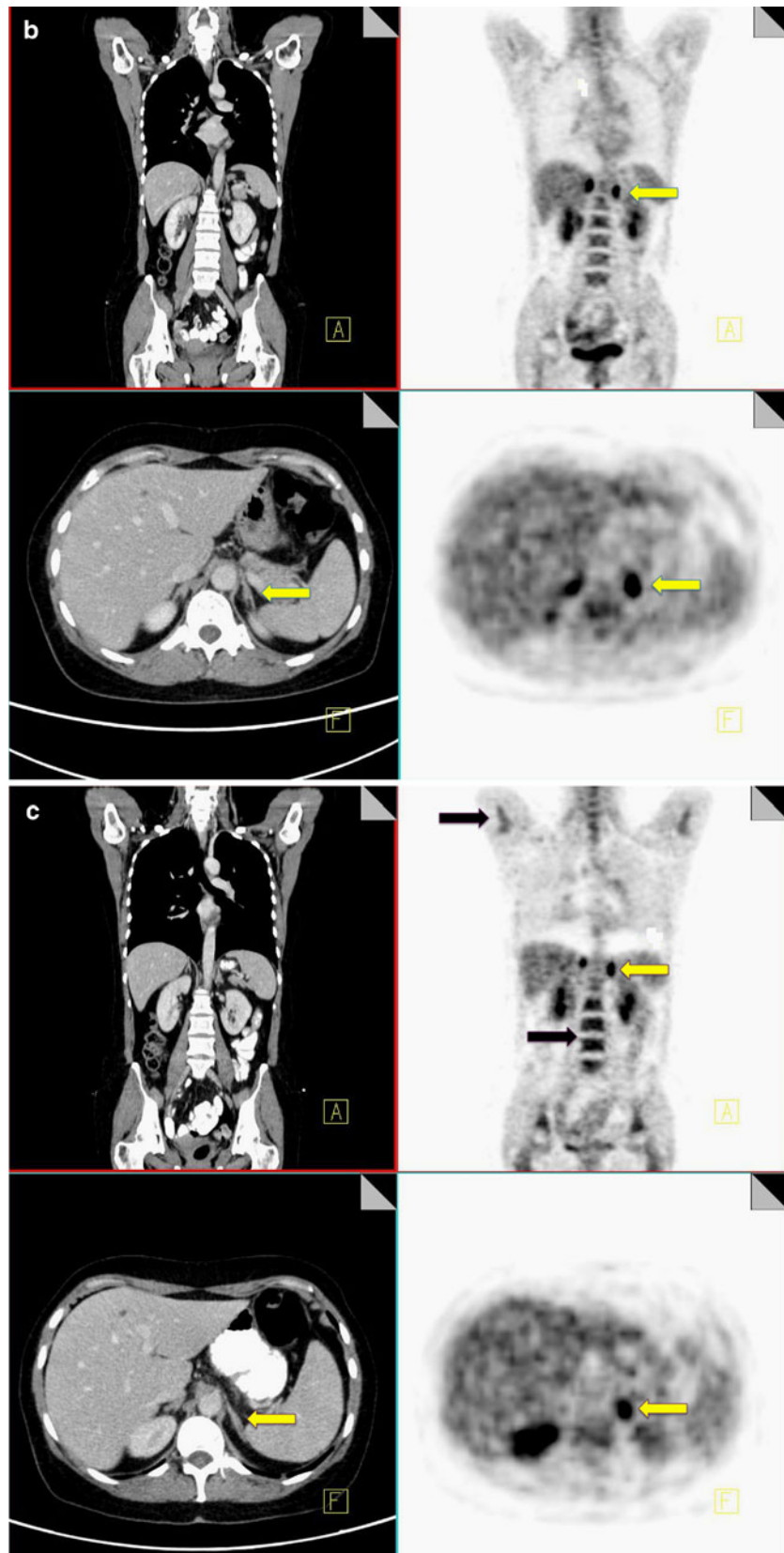
Fig. 6 (continued)

FDG uptake in brown fat has been reported as between 2.5–4% [15, 16].

Hypermetabolic brown fat is more commonly identified in children than in adults and is more prevalent in females than in males. It occurs more frequently in patients with low body mass index and in cold weather [15].

Glucose accumulation within brown fat is increased by sympathetic stimulation as brown fat is innervated by the sympathetic nervous system. In view of this, administration of oral propranolol is advised by some authors as it has been shown to reduce the uptake of FDG by brown fat [17]. This is not performed at our institution; however, attempts are made to reduce FDG uptake in brown fat by maintaining a warm ambient temperature and providing patients with blankets during the uptake phase.

The typical distribution of brown fat in a bilateral symmetric pattern in the supraclavicular and neck regions is rarely confused with malignancy. In cases where hypermetabolic brown fat is seen to surround lymph nodes, the CT images should be separately evaluated to allow morphological assessment of the lymph nodes. The classical CT features of pathological replacement of lymph nodes should be sought, namely increased short axis diameter, loss of the fatty hilum and loss of the normal concavity of the lymph node. If the morphology of the lymph node is entirely normal, malignancy can be confidently excluded and the increased uptake attributed to brown fat [18].

Atypical brown fat in the mediastinum can be misinterpreted as nodal metastases and has been identified in the paratracheal, paraoesophageal, prevascular regions, along the pericardium and in the interatrial septum. Extramediastinal sites of brown fat uptake include the paravertebral regions, perinephric, perihepatic and subdiaphragmatic regions and in the intraatrial septum [16].

The absence of an anatomical lesion on CT imaging in areas of FDG uptake should raise the possibility of brown fat to the reader. Careful evaluation of the CT images must be performed to confirm the presence of adipose tissue in the anatomical region correlating to the increased FDG activity on ^{18}F-FDG PET before this activity be attributed to brown fat.

An awareness of the possibility of brown fat in atypical locations is vital to avoid overstaging, and correlation with CT imaging increases reader confidence in differentiating brown fat from malignancy (Fig. 4).

Uterine and ovarian uptake In premenopausal women endometrial uptake of FDG varies cyclically and is increased both at ovulation and during the menstrual phase of the cycle with mean SUV values of 3.5–5 [19]. Endometrial uptake in postmenopausal women is abnormal and warrants further investigation; however benign explan-

ations for increased FDG uptake include recent curettage, uterine fibroids and endometrial polyps [19].

Benign ovarian uptake of FDG in premenopausal women can be associated with ovulation. In postmenopausal women, ovarian uptake of FDG should be further investigated (Fig. 5).

Adrenal uptake ^{18}F-FDG PET imaging is commonly used for evaluation of adrenal masses in patients with diagnosed malignancies. Similarly incidental adrenal lesions are commonly identified on staging ^{18}F-FDG PET-CT imaging. The positive predictive value of ^{18}F-FDG PET-CT evaluation of adrenal lesions has been reported as high as 95% with a similarly high negative predictive value of 94% [20].

Causes of false-positive adrenal lesions include angiomyolipoma, adrenal hyperplasia and adrenal adenomas (up to 5%) [21, 24]. FDG activity greater than that of the liver is generally associated with malignancy; however benign lesions have been reported with greater activity than liver [21].

Evaluation of the CT component can provide additional diagnostic information with identification of HU attenuation values of <10 on noncontrast CT for adrenal adenomas or fat-containing myelolipomata [21].

Symmetrical intense FDG activity with no identifiable abnormality on CT is associated with benign physiological FDG uptake (Fig. 6).

Thyroid uptake

Thyroid uptake is incidentally identified on ^{18}F-FDG PET imaging with a frequency of almost 4%, with a diffuse uptake pattern in roughly half of cases and a focal pattern in the remainder [22]. The majority of diffuse uptake represents chronic thyroiditis, multinodular goiter or Graves' disease, whereas focal uptake is associated with a risk of malignancy that ranges from 30.9–63.6% in published studies [22, 23]. Focal thyroid uptake requires further investigation with ultrasound and tissue biopsy.

Uptake in the gastrointestinal tract

The pattern of physiological uptake within the GI tract is highly variable. Low-grade linear uptake is likely related to smooth muscle activity and swallowed secretions. More focal increased uptake in the distal esophagus is sometimes seen with Barrett's esophagus. In view of this, referral for OGD may be reasonable in cases of increased uptake in the distal esophagus [14, 24].

The typical pattern of FDG uptake in the stomach is of low-grade activity in a J-shaped configuration. Small bowel typically demonstrates mild heterogeneous uptake throughout. Common pitfalls of small bowel evaluation relate to

spuriously high uptake in underdistended or overlapping loops of bowel [14, 25].

Within the colon, FDG uptake is highly variable, however can be quite avid particularly in the cecum, right colon and rectosigmoid regions. Focal areas of FDG activity within the colon that are of greater intensity than background liver uptake should raise the suspicion of a colonic neoplasm (Fig. 7) [25, 26].

In a review of over 3,000 patients' focal areas of abnormal FDG uptake within the gastrointestinal tract (GIT) were identified in 3% of cases of staging ^{18}F-FDG PET-CT studies.

Incidental malignant lesions were identified in 19% of these patients with pre-malignant lesions including adenomas in 42% of the patients [27]. In view of this endoscopy referral is recommended in the absence of a clear benign correlate for focal areas of avid uptake on CT imaging.

Treatment-related causes of false-positive uptake

There are a number of conditions that can occur in patients undergoing treatment for cancer. When imaging these patients to assess for response, we often see these

treatment-related conditions. It is important to recognize the imaging features to avoid misdiagnosis.

Thymus/thymic hyperplasia

Thymic hyperplasia post-chemotherapy is a well-described phenomenon. It is generally seen in children and young adults at a median of 12 months post chemotherapy [28]. The presence of increased FDG uptake in the anterior mediastinum can be attributed to thymic hyperplasia by identification of a triangular soft tissue density seen retrosternally on CT with a characteristic bilobed anatomical appearance [29]. In the presence of thymic hyperplasia, there is generally preservation of the normal shape of the gland despite an increase in size [30].

Superior mediastinal extension of thymic tissue is an anatomical variant that has been described in children and young adults (Fig. 8).

It presents as a soft tissue nodule anteromedial to the left brachiocephalic vein and represents a remnant of thymic tissue along the path of migration in fetal life. In patients with thymic hyperplasia, a superior mediastinal nodule in this location may represent accessory thymic tissue. An


Fig. 7 ^{18}F-FDG PET-CT restaging scan performed in a 65-year-old female with a history of breast cancer. Incidental focal uptake is identified in the ascending colon where some abnormal thickening is seen on the CT component (yellow arrow). Colonoscopy confirmed the presence of a T3 adenocarcinoma
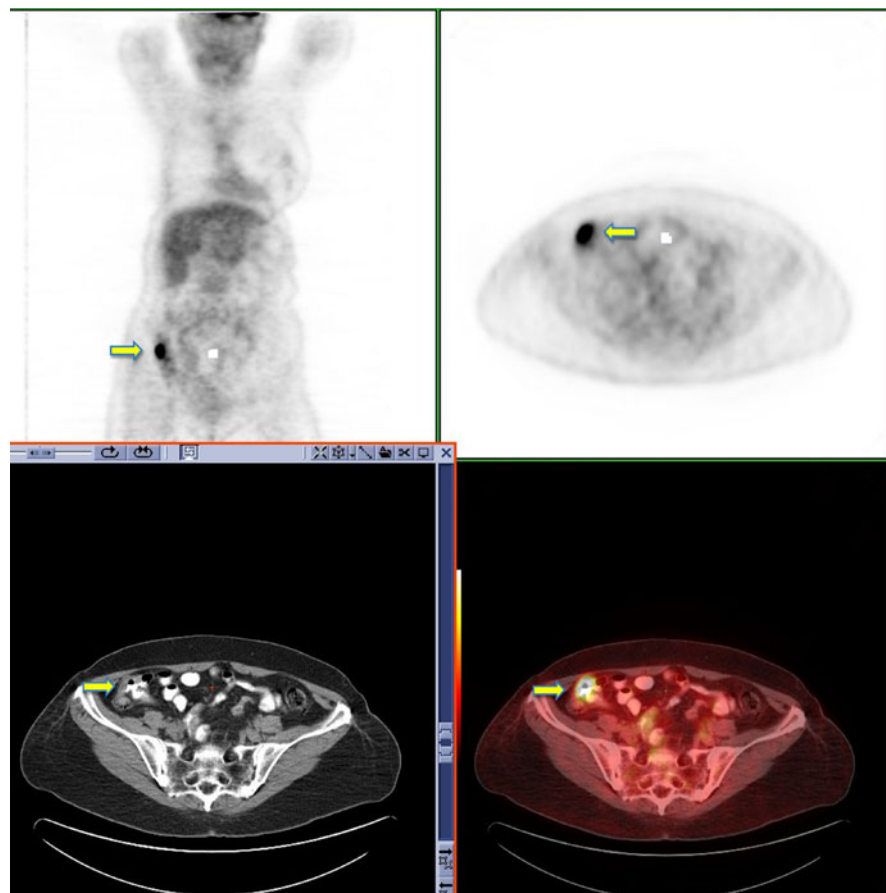
Fig. 8 A 3.5-year-old boy with abdominal Burkitt's lymphoma. Coronal ¹⁸F-FDG PET scan obtained 5 months after completion of treatment shows increased activity in the thymus in an inverted V configuration and in superior thymic extension (white arrow). Note physiologic activity within the right neck in the sternocleidomastoid muscle (a). Axial CT image from the same ¹⁸F-FDG PET-CT study performed 5 months after treatment shows a nodule (white arrow) anteromedial to the left brachiocephalic vein (b). Axial fusion image shows that the FDG activity in the superior mediastinum corresponds to this enlarged nodule anteromedial to left brachiocephalic vein (white arrow) (c). Axial fusion image shows increased activity in an enlarged thymus consistent with thymic hyperplasia (white arrow; standardized uptake value 3.0) of similar intensity to activity in superior mediastinum (d)
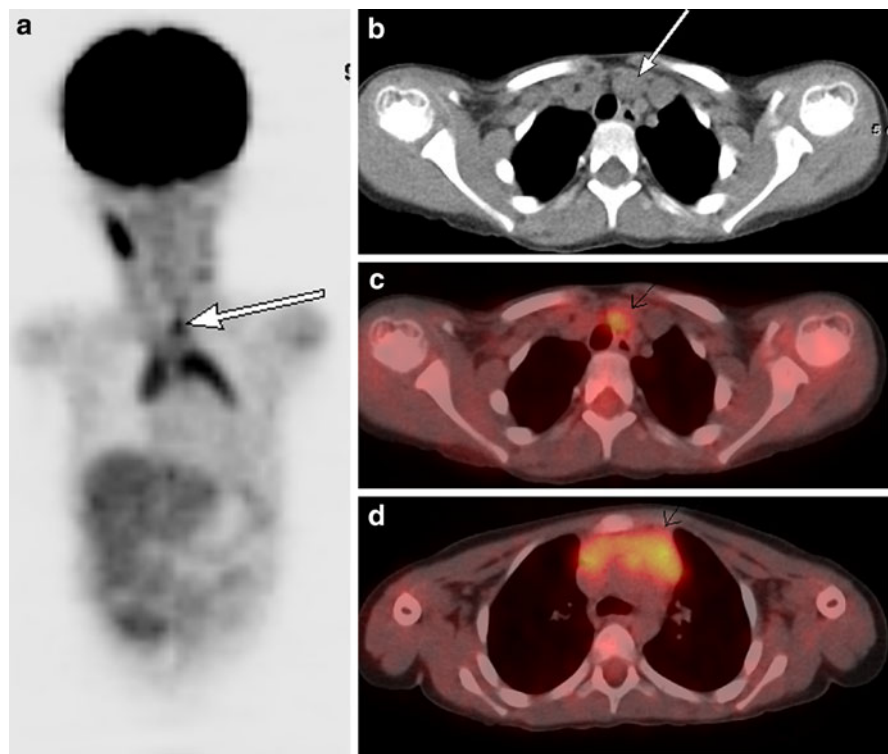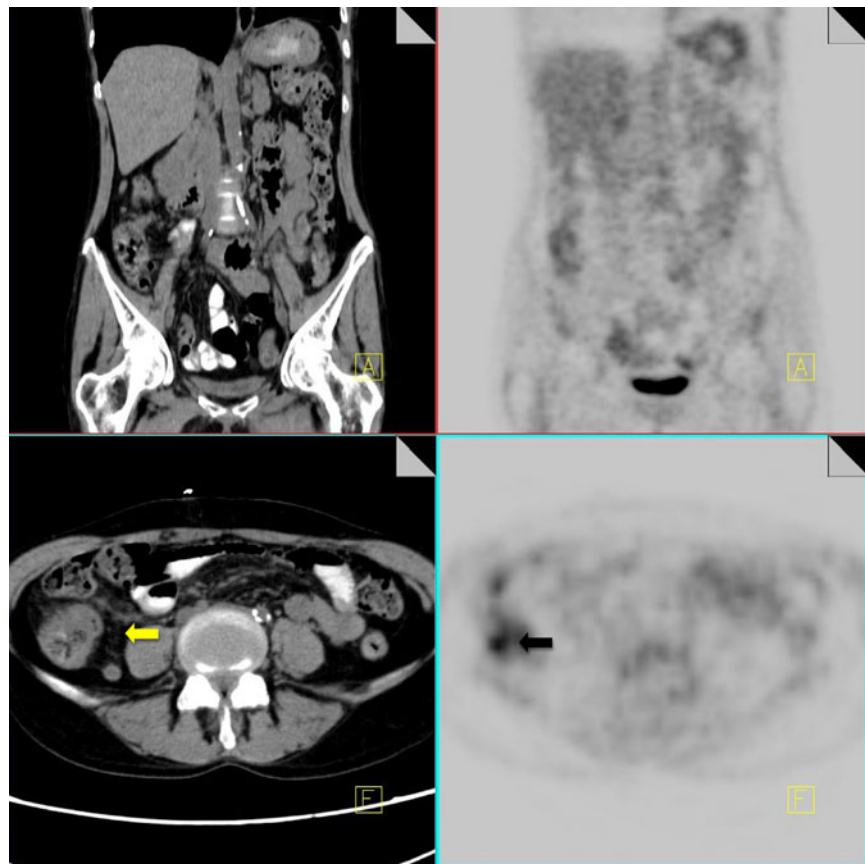

Fig. 9 ¹⁸F-FDG PET-CT performed in a 46-year-old male post four cycles of chemotherapy for lymphoma and 2 weeks post administration of G-CSF. Note the diffuse homogeneous increased uptake throughout the bone marrow and the increased uptake in the spleen (yellow arrow)
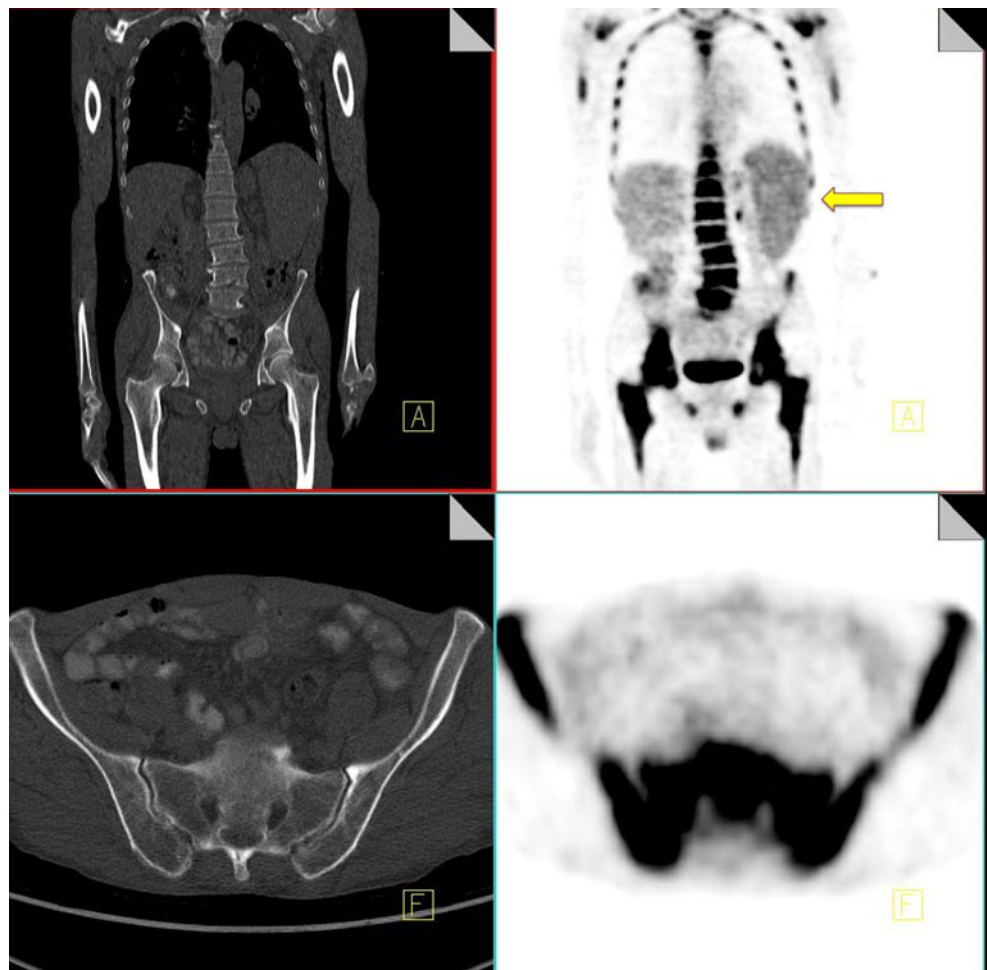
Fig. 10 [18]F18-FDG PET-CT performed in a 52-year-old male with newly diagnosed esophageal carcinoma. Increased FDG uptake is identified within the esophagus (black arrow) and an upper abdominal lymph node (yellow arrow), consistent with malignancy (**a**). [18]F18-FDG PET-CT performed 6 weeks post-completion of radiotherapy for esophageal carcinoma. Linear increased uptake is identified along the mediastinum in the radiation port (black arrow). This corresponds to areas of ground-glass change on CT (yellow arrow) consistent with acute radiation change (**b**)
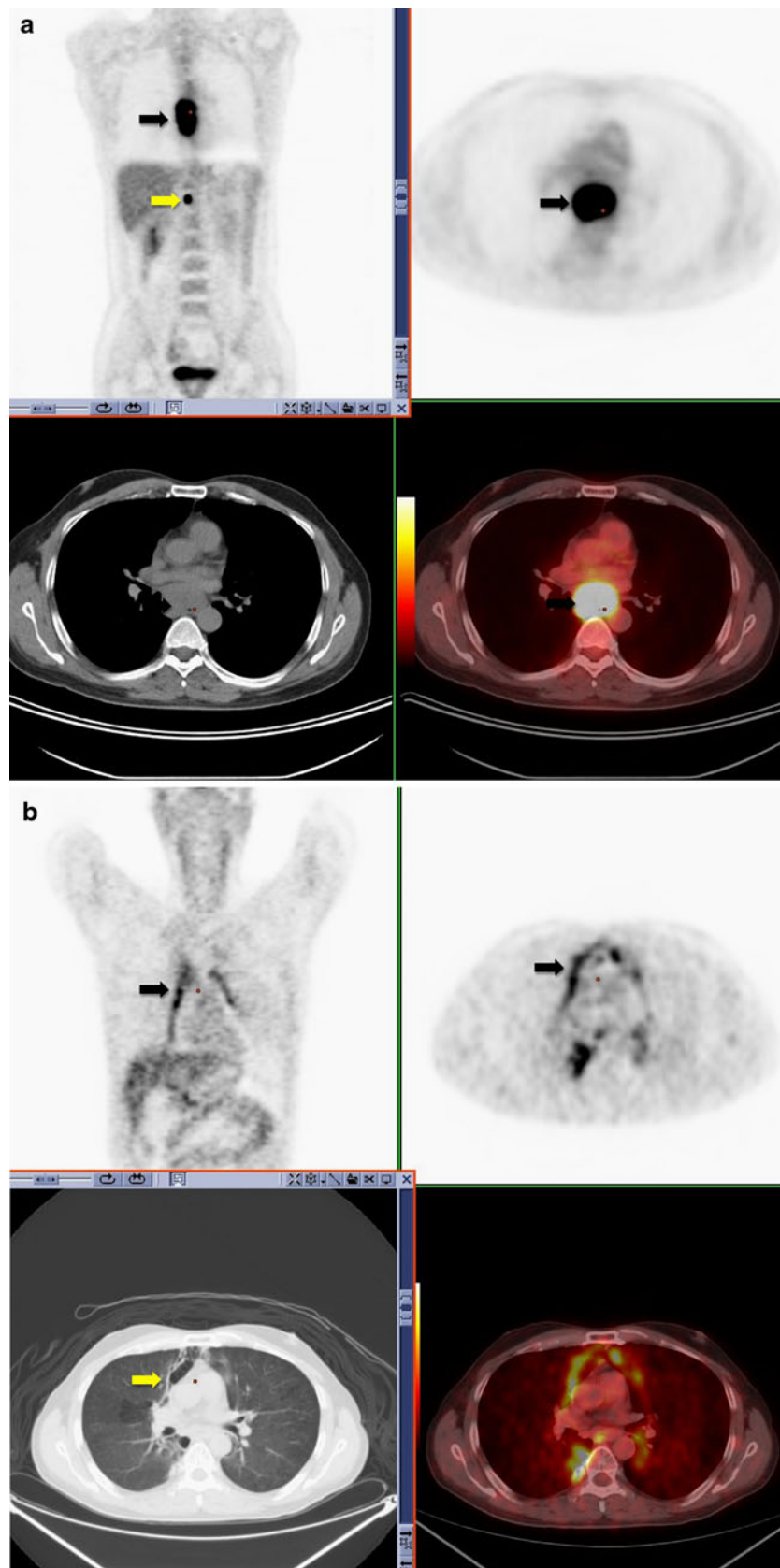
Fig. 11 ^{18}F-FDG PET-CT performed in a 57-year-old male 2 weeks following chemotherapy for lung cancer. Increased FDG uptake is noted within the cecum (black arrow). On CT there is some thickening of the cecal wall and stranding of the pericecal fat (yellow arrow) consistent with typhilits

Fig. 12 ^{18}F-FDG PET-CT performed in a 69-year-old male with a history of non-Hodgkin's lymphoma. The patient had a previous talc pleurodesis for a persistent left pleural effusion. Increased FDG activity is identified within the left pleura (black arrow). CT demonstrates a pleural effusion with high density material along the left pleural surface consistent with talc (yellow arrow)
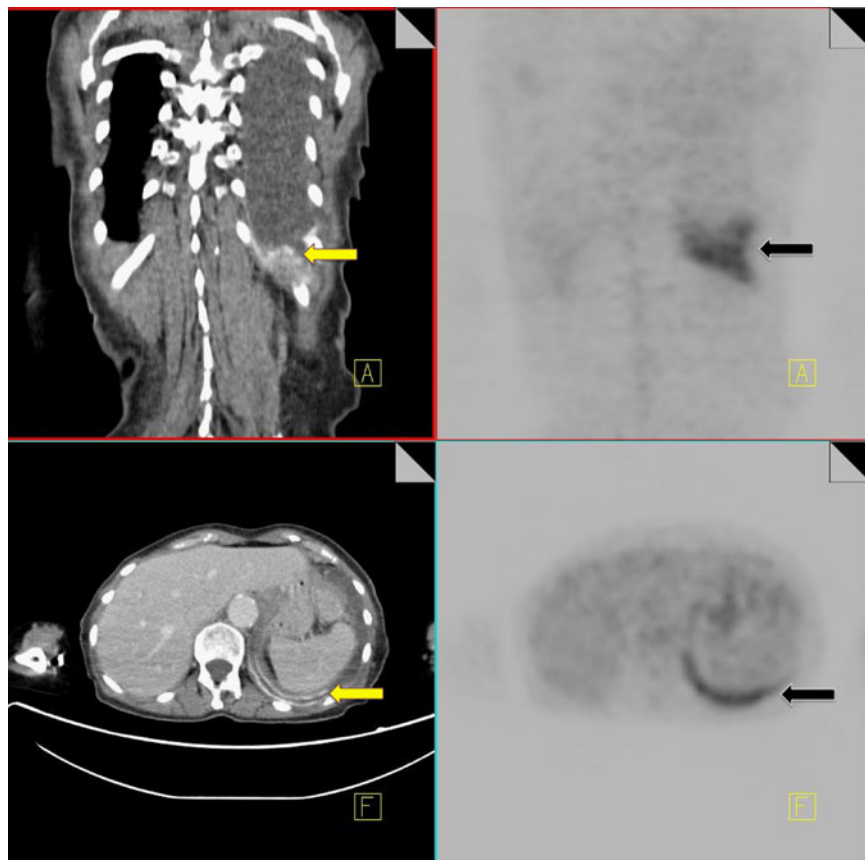
awareness of this physiological variant is necessary to prevent misdiagnosis [28].

G-CSF changes

Granulocyte colony-stimulating factor is a glycoprotein hormone that regulates proliferation and differentiation of granulocyte precursors. It is used to accelerate recovery from chemotherapy-related neutropaenia in cancer patients. Intense increased FDG uptake is commonly observed in the bone marrow and spleen following GCSF therapy; however the bone marrow response to GCSF can be differentiated from pathological infiltration by its intense homogeneous nature without focally increased areas of FDG uptake. Increased FDG uptake attributable to GCSF uptake rapidly decreases following completion of therapy and generally resolves within a month (Fig. 9).

Marked uptake in the bone marrow can also be seen following chemotherapy, reflecting marrow activation [31, 32].

Radiation pneumonitis Inflammatory morphological changes in the radiation field post-irradiation of primary or metastatic lung tumor can result in false-positive diagnosis. Radiation pneumonitis typically occurs following high doses of external beam radiotherapy (>40 Gy). In the acute phase (1–8 weeks) radiation pneumonitis is characterized by ground-glass opacities and patchy consolidation. This can commonly lead to a misdiagnosis of infection. Chronic CT appearances of fibrosis and traction bronchiectasis in the radiation field allow correct interpretation of increased FDG uptake as radiation pneumonitis as opposed to disease recurrence [33, 34]. Other organs are also sensitive to radiation, and persistent uptake due to inflammatory change can persist for up to 1 year. It is important to elicit a history of radiation from the patient and to correlate the increased uptake with the CT findings to avoid missing a disease recurrence (Fig. 10).

Infection

Bone marrow suppression places chemotherapy patients at increased risk of infection.

Fig. 13 ^{18}F-FDG PET-CT performed in a 46-year-old gentleman with a history of non-Hodgkin's lymphoma. Increased FDG uptake is identified in the right proximal humerus (black arrow). CT of the area demonstrates a corresponding vague area of sclerosis (yellow arrow). Biopsy of the area yielded osteonecrosis with no evidence of metastatic disease
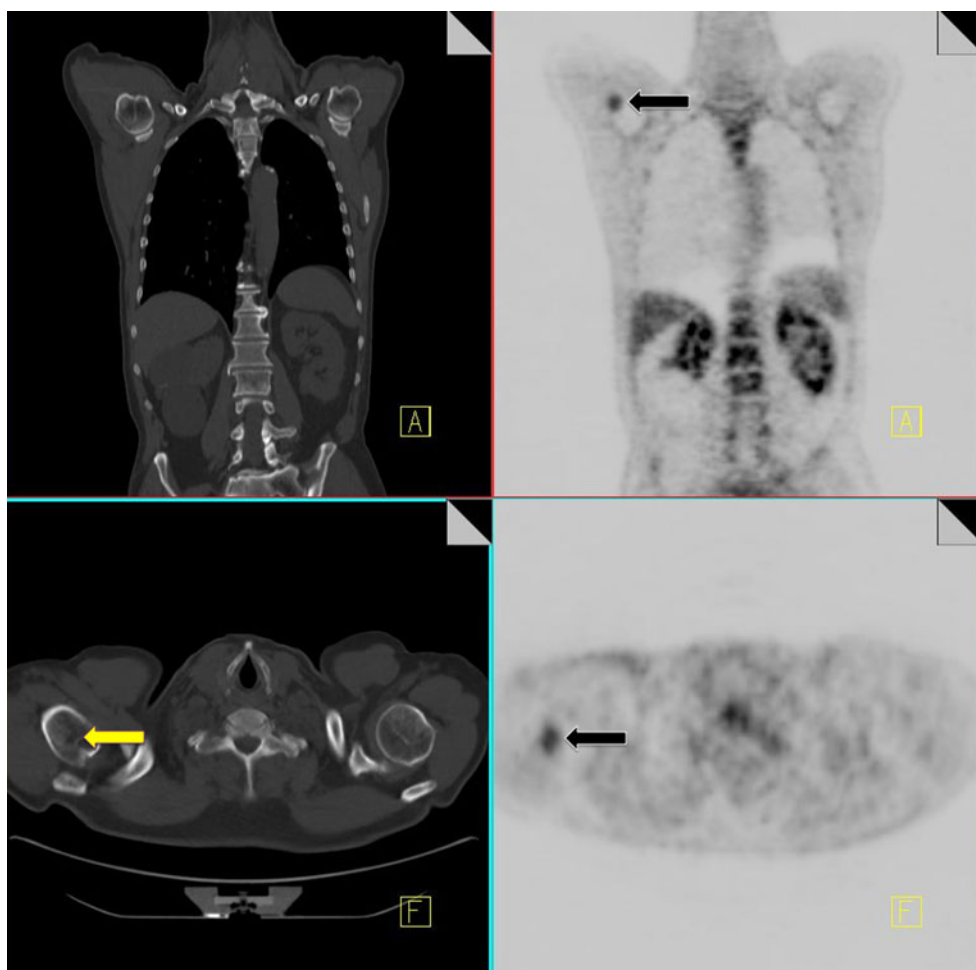
Inflammatory cells such as neutrophils and activated macrophages at the site of infection or inflammation actively accumulate FDG [35].

In the post-therapy setting it has been reported that up to 40% of FDG uptake occurs in non-tumor tissue [12]. Infection is one of the most common causes of false-positive ^{18}F-FDG PET-CT findings post-chemotherapy. Chemotherapy patients are susceptible to a wide variety of infections, including upper respiratory chest infections, pneumonia, colitis and cholecystitis. Reactivation of tuberculous infection can occur in immunocompromised patients post,chemotherapy, and correlation with CT imaging can prevent misdiagnosis in suspected cases.

Atypical infections such as cryptococcosis and pneumocystis can also present as false-positives on FDG imaging (Fig. 11) [36].

Surgery and radiotherapy

There are inherent challenges in the interpretation of ^{18}F-FDG PET-CT imaging in the postoperative patient. Non-tumor-related uptake of FDG is frequently identified in post-operative wound sites, at colostomy sites or at the site

of post-radiation inflammatory change. ^{18}F-FDG PET-CT imaging during the early postoperative/post-radiotherapy period may result in overstaging of patients because of non-neoplastic uptake of FDG [12]. Careful evaluation of the CT component in this setting is vital as CT imaging can provide valuable additional information regarding benign inflammatory conditions commonly encountered in the postoperative setting such as abscesses or wound infection. These conditions are often readily apparent on CT, particularly when oral and/or IV contrast CT is administered.

The reader should also bear in mind that avid uptake of FDG at postoperative/post radiotherapy sites may mask malignant FDG uptake in neighboring structures. In order to minimize non-tumoral uptake of FDG, it is advisable to allow at least 6 weeks post-surgery or completion of radiotherapy prior to performing staging ^{18}F-FDG PET-CT [24].

Talc pleurodesis Talc pleurodesis is a commonly performed procedure for the treatment of persistent pneumothorax or pleural effusion. The fibrotic/inflammatory reaction results in increased FDG uptake on ^{18}F-FDG PET imaging with corresponding high-density areas of pleural thickening on

Fig. 14 ^{18}F-FDG PET-CT performed in a 46-year-old female, 3 years post-chemo-radiation for cervical carcinoma. Low grade FDG uptake is identified in the left acetabulum and right pubic bone (black arrow). CT demonstrates pathological fractures in these areas consistent with insufficiency fractures (yellow arrow)
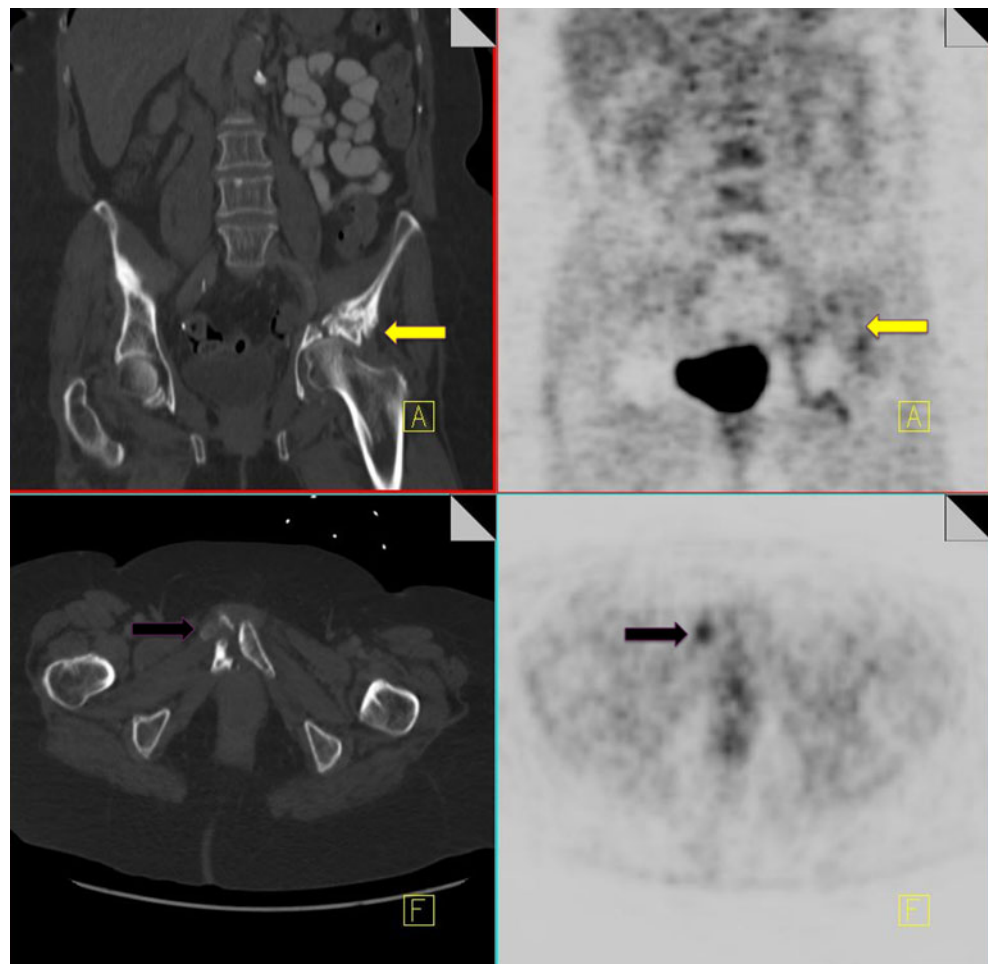
CT. SUV values of between 2–16.3 have been seen years after the procedure [37].

When increased FDG uptake is indentified in the pleural space in a patient with a known history of pleurodesis, correlation with CT is recommended to detect pleural thickening of increased attenuation that suggests talc rather than tumor.

It is extremely important that a comprehensive history with relevant surgical interventions is available to the reader in order to ensure accurate diagnosis and staging (Fig. 12).

Flare phenomenon Bone healing is mediated by osteoblasts, and an early increase in osteoblast activity on successful treatment of metastatic disease has been described [38]. "Bone flare" refers to a disproportionate increase in bone lesion activity on isotope bone scan despite evidence of a therapeutic response to treatment in other lesions and has been well described in breast, prostate and lung tumors. 'Flare phenomenon' has also

been described on ^{18}F-FDG PET-CT in patients with lung and breast cancer who are receiving chemotherapy [39].

Differentiating between increased FDG uptake due to flare response and true disease progression may not be possible in the early post-treatment studies. While it is recognized that bone flare is a rare phenomenon, an increase in baseline skeletal activity and appearance of new bone lesions despite apparent response or stable disease elsewhere should be interpreted with caution to avoid erroneously suggesting progressive disease.

Osteonecrosis Osteonecrosis or avascular necrosis has been well described as a complication of combination chemotherapy treatment, especially where it includes intermittent high-dose corticosteroids (e.g., lymphoma patients) [40]. Commonly encountered sites include the hip and less frequently the proximal humerus. Occasionally we can see a discrete entity known as jaw osteonecrosis. Patients receiving IV bisphosphonates for the management of bone

Fig. 15 ^{18}F-FDG PET-CT performed in a 67-year-old male for restaging of laryngeal carcinoma. Increased FDG uptake is noted in the left lower neck and left mediastinum (black arrow). CT demonstrates lymphadenopathy in these areas (yellow arrow), some of which are calcified. Biopsy of the left lower neck node confirmed sarcoidosis
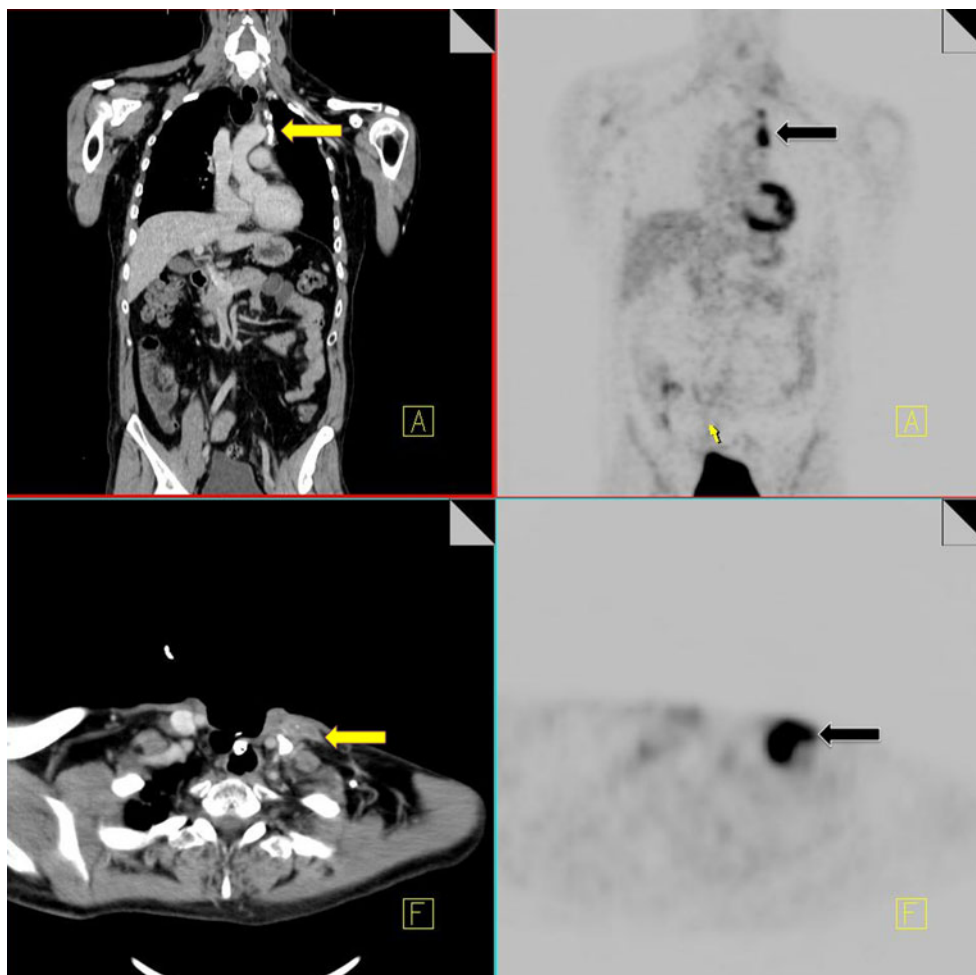
Fig. 16 ^{18}F-FDG PET-CT performed in a 52-year-old female with breast cancer and chronic hepatitis. On the CT component a hyper-enhancing mass is identified in segment 4 of the liver (yellow arrow). No increased FDG activity is identified in this area on the PET component. Biopsy of the mass confirmed the diagnosis of a hepatocellular carcinoma
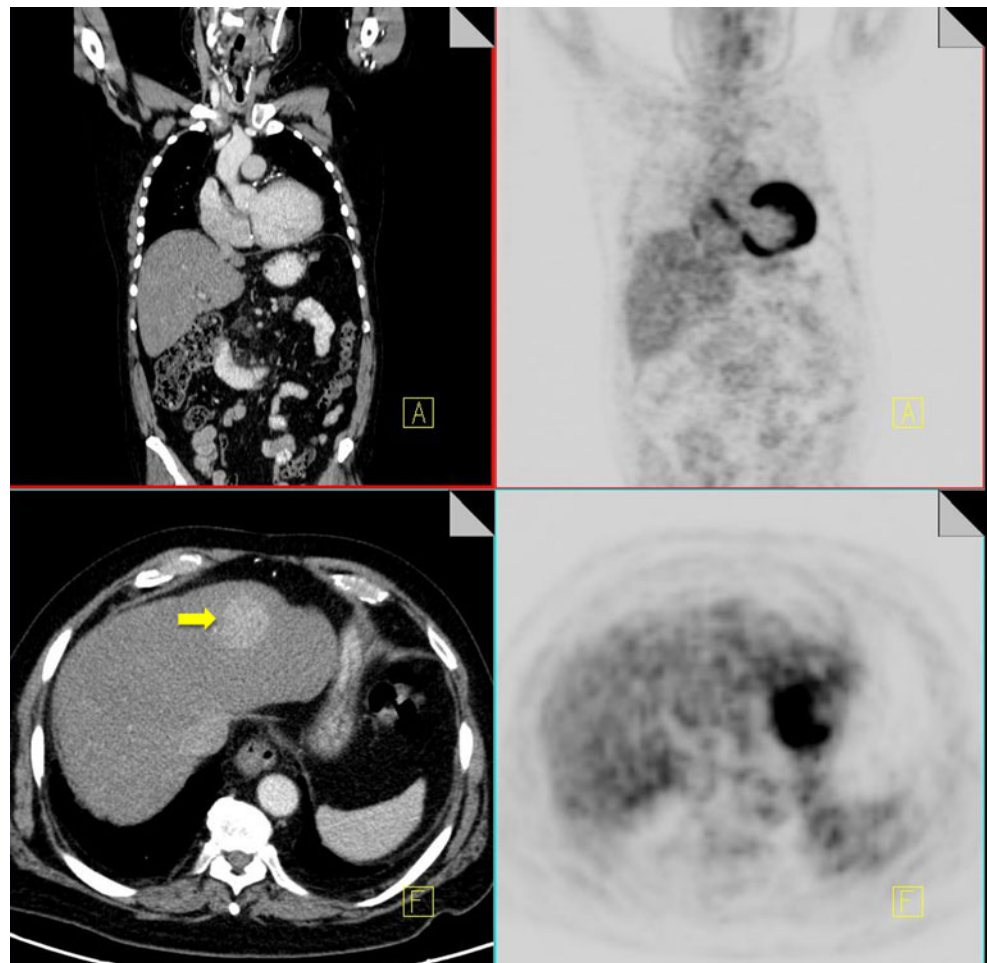
metastases are at an increased risk of developing this [41]. The development of osteonecrosis in the mandible is frequently preceded by tooth extraction. Radiographic findings that may be visualized on CT include osteosclerosis, dense woven bone, thickened lamina dura and sub-periosteal bone deposition [42]. FDG uptake can be seen in areas of osteonecrosis (Fig. 13).

Insufficiency fractures Pelvic insufficiency fractures have been described following irradiation for gynecological, colorectal, anal and prostate cancer. They commonly occur within 3–12 months post-radiation treatment, and osteoporosis is often a precipitating factor. FDG uptake in insufficiency fractures ranges from mild and diffuse to intense and heterogeneous. The maximum SUV values are variable with reported values of between 2.4–7.2 [43]. Differentiating insufficiency fractures from bone metastases can prove challenging; however they are often bilateral and occur in characteristic locations within the radiation field—sacral ala, pubic rami and iliac bones. Biopsy of insufficiency fractures can lead to irreparable damage and so

careful correlation of ^{18}F-FDG PET imaging with the CT component along with radiation history is vital for correct diagnosis. CT allows evaluation of the bone cortex and adjacent soft tissues, which can confirm the diagnosis of a pathological fracture or a metastatic deposit.

Follow-up of suspected insufficiency fractures demonstrates a reduction in FDG uptake over time (Fig. 14) [43].

Sarcoidosis Sarcoidosis is a chronic multisystem disorder characterized by non-caseating granulomas and derangement of normal tissue architecture [36]. Sarcoidosis has been reported in association with a variety of malignancies either synchronously or post-chemotherapy. Aggregation of inflammatory cells post-chemotherapy is associated with accumulation of FDG, and the intensity of FDG uptake may correlate with disease activity [36].

When suspected disease recurrence presents with signs and symptoms compatible with sarcoidosis (i.e., mediastinal and bihilar lymphadenopathy), this must be excluded by clinical, radiological and pathological correlation to prevent mistreatment (Fig. 15).
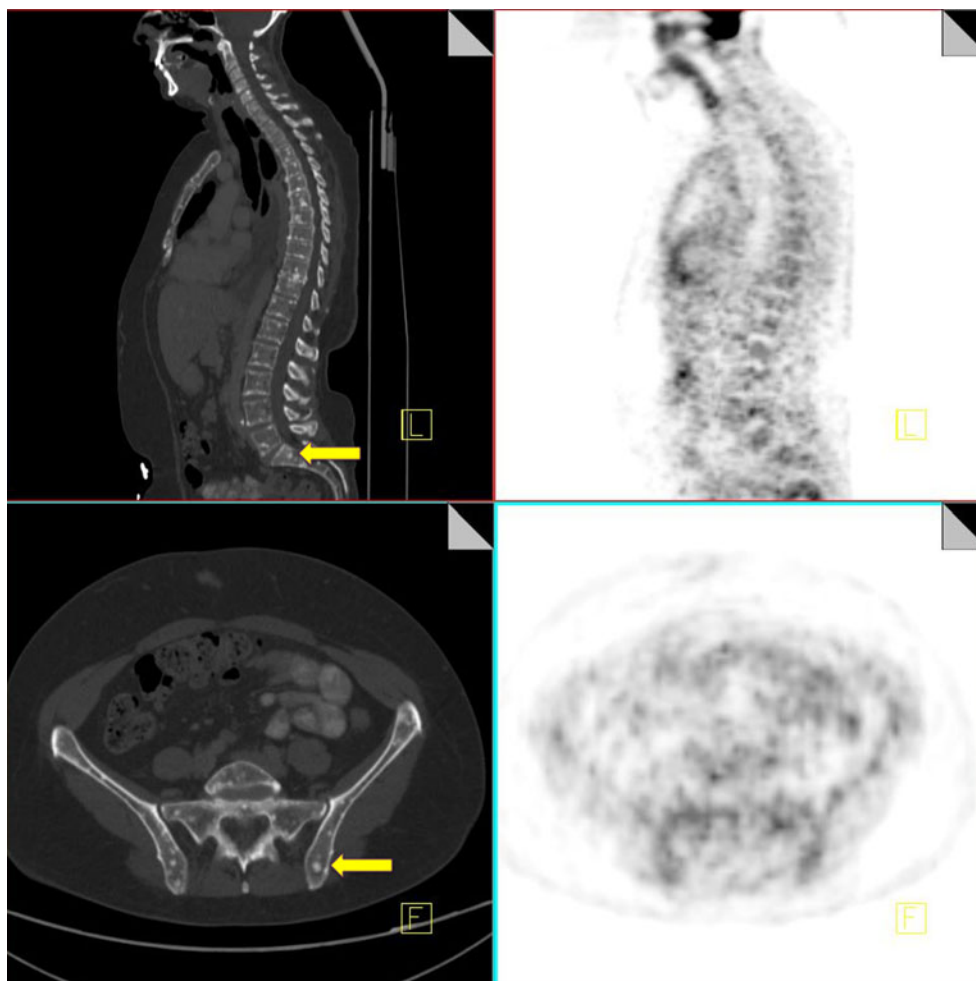
FDG-PET negative tumors

There are a number of malignancies that can be FDG-PET negative. Examples include bronchoalveolar carcinoma and carcinoid tumors in the lung, renal cell carcinomas and hepatomas, mucinous tumors of the GIT and colon, and low grade lymphomas [3, 44–48]. Careful evaluation of the CT component of the study however will prevent a misdiagnosis (Fig. 16).

Osteoblastic metastases

Bone metastases are diagnosed in up to 85% of patients with advanced breast cancer, leading to significant morbidity and mortality. Sclerotic bone metastases are commonly associated with breast carcinoma [49]. ^{18}F-FDG PET imaging is superior to nuclear bone scan in detection of osteolytic breast metastases; however it commonly fails to diagnose osteoblastic or sclerotic metastases [50]. Review of bony windows on CT imaging allows identification of sclerotic metastases and ensures accurate staging of metastatic bone disease (Fig. 17).

Discussion/conclusion

^{18}F-FDG PET imaging has dramatically changed cancer staging, and findings of restaging studies commonly effect changes in treatment protocols. ^{18}F-FDG however is not tumor specific. As interpreting physicians we need to be aware of these false positives and false negatives. In this review we have outlined atypical physiological sites of FDG uptake along with common causes of FDG uptake in benign pathological conditions, many of which are treatment related. With ^{18}F-FDG PET-CT we have the advantage of two imaging modalities. The PET component gives us functional information and the CT, anatomical data. We have discussed the importance of dual-modality imaging and correlation with CT imaging of the above conditions. Furthermore CT imaging provides important diagnostic information in evaluation of tumors that poorly concentrate FDG. In light of the increased reliance of ^{18}F-FDG PET-CT for cancer staging, it is vital that radiologists and nuclear medicine physicians be aware of pitfalls in ^{18}F-FDG PET-CT imaging and correlate PET and CT components to avoid

Fig. 17 Staging ^{18}F-FDG PET-CT performed in a 45-year-old female with newly diagnosed breast cancer. CT demonstrates multiple small sclerotic foci in the spine and pelvis (yellow arrow), consistent with bony metastases. These are FDG negative on the PET component of the study

misdiagnosis, overstaging of disease and unnecessary biopsies.

References

1. Pauwels EK, Ribeiro MJ, Stoot JH et al (1998) FDG accumulation and tumor biology. Nucl Med Biol 25:317–322

2. Wahl RL (1996) Targeting glucose transporters for tumor imaging: "sweet" idea, "sour" result. J Nucl Med 37(6):1038–1041

3. Kim BT, Kim Y, Lee KS, Yoon SB, Cheon EM, Kwon OJ, Rhee CH, Han J, Shin MH (1998) Localized form of bronchioalveolar carcinoma: FDG PET findings. AJR 170(4):935–939

4. Hoh CK, Hawkins RA, Glaspy JA, Dahlbom M, Tse NY, Hoffman EJ, Schiepers C, Choi Y, Rege S, Nitzsche E (1993) Cancer detection with whole-body PET using 2-[18F]fluoro-2-deoxy-D-glucose. J Comput Assist Tomogr 17(4):582–589

5. Fenchel S, Grab D, Nuessle K, Kotzerke J, Rieber A, Kreienberg R, Brambs HJ, Reske SN (2002) Asymptomatic adnexal masses: correlation of FDG PET and histopathologic findings. Radiology 223(3):780–788

6. Shreve PD, Anzai Y, Wahl RL (1999) Pitfalls in oncologic diagnosis with FDG PET imaging: physiologic and benign variants. Radiographics 19(1):61–77, quiz 150–151

7. Abouzied MM, Crawford ES, Nabi HA (2005) 18 F-FDG imaging: pitfalls and artifacts. J Nucl Med Technol 33(3):145–155

8. Boellaard R, O'Doherty MJ, Weber WA, Mottaghy FM, Lonsdale MN, Stroobants SG, Oyen WJ, Kotzerke J, Hoekstra OS, Pruim J, Marsden PK, Tatsch K, Hoekstra CJ, Visser EP, Arends B, Verzijlbergen FJ, Zijlstra JM, Comans EF, Lammertsma AA, Paans AM, Willemsen AT, Beyer T, Bockisch A, Schaefer-Prokop C, Delbeke D, Baum RP, Chiti A, Krause BJ (2010) FDG PET and PET/CT: EANM procedure guidelines for tumour PET imaging: version 1.0. Eur J Nucl Med Mol Imaging 37(1):181–200

9. Sureshbabu W, Mawlawi O (2005) PET/CT imaging artifacts. J Nucl Med Technol 33(3):156–161, quiz 163–164

10. Lin E, Alavi A (2009) PET and PET/CT: A Clinical Guide: 2nd Edn. Thieme New York p 145

11. Hany TF, Heuberger J, von Schulthess GK (2003) Iatrogenic FDG foci in the lungs: a pitfall of PET image interpretation. Eur Radiol 13(9):2122–2127, Epub 2002 Oct 17

12. Kazama T, Faria SC, Varavithya V, Phongkitkarun S, Ito H, Macapinlac HA (2005) FDG PET in the evaluation of treatment for lymphoma: clinical usefulness and pitfalls. Radiographics 25(1):191–207

13. Swanson DP, Chilton HM, Thrall JH (1990) Pharmaceuticals in medical imaging. Macmillan, New York

14. Prabhakar HB, Sahani DV, Fischman AJ, Mueller PR, Blake MA (2007) Bowel hot spots at PET-CT. Radiographics 27(1):145–159

15. Yeung HW, Grewal RK, Gonen M, Schöder H, Larson SM (2003) Patterns of (18)F-FDG uptake in adipose tissue and muscle: a potential source of false-positives for PET. J Nucl Med 44(11):1789–1796

16. Truong MT, Erasmus JJ, Munden RF, Marom EM, Sabloff BS, Gladish GW, Podoloff DA, Macapinlac HA (2004) Focal FDG uptake in mediastinal brown fat mimicking malignancy: a potential pitfall resolved on PET/CT. Am J Roentgenol 183(4):1127–1132

17. Söderlund V, Larsson SA, Jacobsson H (2007) Reduction of FDG uptake in brown adipose tissue in clinical patients by a single dose of propranolol. Eur J Nucl Med Mol Imaging 34(7):1018–1022

18. Sumi M, Ohki M, Nakamura T (2001) Comparison of sonography and CT for differentiating benign from malignant cervical lymph nodes in patients with squamous cell carcinoma of the head and neck. AJR 176(4):1019–1024

19. Lerman H, Metser U, Grisaru D, Fishman A, Lievshitz G, Even-Sapir E (2004) Normal and abnormal 18 F-FDG endometrial and ovarian uptake in pre- and postmenopausal patients: assessment by PET/CT. J Nucl Med 45(2):266–271

20. Lu Y, Xie D, Huang W, Gong H, Yu J (2010) 18 F-FDG PET/CT in the evaluation of adrenal masses in lung cancer patients. Neoplasma 57(2):129–134

21. Boland GW, Blake MA, Holalkere NS, Hahn PF (2009) PET/CT for the characterization of adrenal masses in patients with cancer: qualitative versus quantitative accuracy in 150 consecutive patients. AJR Am J Roentgenol 192(4):956–962

22. Chen W, Parsons M, Torigian DA, Zhuang H, Alavi A (2009) Evaluation of thyroid FDG uptake incidentally identified on FDG-PET/CT imaging. Nucl Med Commun 30(3):240–244

23. Choi JY, Lee KS, Kim HJ, Shim YM, Kwon OJ, Park K, Baek CH, Chung JH, Lee KH, Kim BT (2006) Focal thyroid lesions incidentally identified by integrated 18 F-FDG PET/CT: clinical significance and improved characterization. J Nucl Med 47(4):609–615

24. Blake MA, Slattery J, Sahani DV, Kalra MK (2005) Practical issues in abdominal PET/CT. Appl Radiol 34(11):8–18

25. Kei PL, Vikram R, Yeung HW, Stroehlein JR, Macapinlac HA (2010) Incidental finding of focal FDG uptake in the bowel during PET/CT: CT features and correlation with histopathologic results. AJR Am J Roentgenol 194(5):W401–W406

26. Pandit-Taskar N, Schöder H, Gonen M, Larson SM, Yeung HW (2004) Clinical significance of unexplained abnormal focal FDG uptake in the abdomen during whole-body PET. AJR Am J Roentgenol 183(4):1143–1147

27. Kamel EM, Thumshirn M, Truninger K, Schiesser M, Fried M, Padberg B, Schneiter D, Stoeckli SJ, von Schulthess GK, Stumpe KD (2004) Significance of incidental 18 F-FDG accumulations in the gastrointestinal tract in PET/CT: correlation with endoscopic and histopathologic results. J Nucl Med 45(11):1804–1810

28. Smith CS, Schöder H, Yeung HW (2007) Thymic extension in the superior mediastinum in patients with thymic hyperplasia: potential cause of false-positive findings on 18 F-FDG PET/CT. AJR Am J Roentgenol 188(6):1716–1721

29. Ferdinand B, Gupta P, Kramer EL (2004) Spectrum of thymic uptake at 18 F-FDG PET. Radiographics 24(6):1611–1616

30. Baron RL, Lee JK, Sagel SS, Levitt RG (1982) Computed tomography of the abnormal thymus. Radiology 142(1):127–134

31. Hollinger EF, Alibazoglu H, Ali A, Green A, Lamonica G (1998) Hematopoietic cytokine-mediated FDG uptake simulates the appearance of diffuse metastatic disease on whole-body PET imaging. Clin Nucl Med 23(2):93–98

32. Kazama T, Swanston N, Podoloff DA, Macapinlac HA (2005) Effect of colony-stimulating factor and conventional- or high-dose chemotherapy on FDG uptake in bone marrow. Eur J Nucl Med Mol Imaging 32(12):1406–1411

33. Claude L, Pérol D, Ginestet C, Falchero L, Arpin D, Vincent M, Martel I, Hominal S, Cordier JF, Carrie C (2004) A prospective study on radiation pneumonitis following conformal radiation therapy in non-small-cell lung cancer: clinical and dosimetric factors analysis. Radiother Oncol 71(2):175–181

34. Frank A, Lefkowitz D, Jaeger S, Gobar L, Sunderland J, Gupta N, Scott W, Mailliard J, Lynch H, Bishop J et al (1995) Decision logic for retreatment of asymptomatic lung cancer recurrence based on positron emission tomography findings. Int J Radiat Oncol Biol Phys 32(5):1495–1512

35. Love C, Tomas MB, Tronco GG, Palestro CJ (2005) FDG PET of infection and inflammation. Radiographics 25(5):1357–1368

36. Chang JM, Lee HJ, Goo JM, Lee HY, Lee JJ, Chung JK, Im JG (2006) False positive and false negative FDG-PET scans in various thoracic diseases. Korean J Radiol 7(1):57–69

37. Kwek BH, Aquino SL, Fischman AJ (2004) Fluorodeoxyglucose positron emission tomography and CT after talc pleurodesis. Chest 125(6):2356–2360

38. Coleman RE, Mashiter G, Whitaker KB, Moss DW, Rubens RD, Fogelman I (1988) Bone scan flare predicts successful systemic therapy for bone metastases. J Nucl Med 29(8):1354–1359

39. Krupitskaya Y, Eslamy HK, Nguyen DD, Kumar A, Wakelee HA (2009) Osteoblastic Bone Flare on F18-FDG PET in Non-small Cell Lung Cancer (NSCLC) Patients Receiving Bevacizumab in addition to standard Chemotherapy. J Thorac Oncol 4(3):429–431

40. Talamo G, Angtuaco E, Walker RC, Dong L, Miceli MH, Zangari M, Tricot G, Barlogie B, Anaissie E (2005) Avascular necrosis of femoral and/or humeral heads in multiple myeloma: results of a prospective study of patients treated with dexamethasone-based regimens and high-dose chemotherapy. J Clin Oncol 23(22):5217–5223

41. Catalano L, Del Vecchio S, Petruzziello F, Fonti R, Salvatore B, Martorelli C, Califano C, Caparrotti G, Segreto S, Pace L, Rotoli B (2007) Sestamibi and FDG-PET scans to support diagnosis of jaw osteonecrosis. Ann Hematol 86(6):415–423

42. Arce K, Assael LA, Weissman JL, Markiewicz MR (2009) MR imaging findings in bisphosphonate-related osteonecrosis of jaws. J Oral Maxillofac Surg 67(5 Suppl):75–84

43. Oh D, Huh SJ, Lee SJ, Kwon JW (2009) Variation in FDG uptake on PET in patients with radiation-induced pelvic insufficiency fractures: a review of 10 cases. Ann Nucl Med 23(6):511–516

44. Erasmus JJ, McAdams HP, Patz EF Jr, Coleman RE, Ahuja V, Goodman PC (1998) Evaluation of primary pulmonary carcinoid tumors using FDG PET. AJR Am J Roentgenol 170(5):1369–1373

45. Kang DE, White RL Jr, Zuger JH, Sasser HC, Teigland CM (2004) Clinical use of fluorodeoxyglucose F 18 positron emission tomography for detection of renal cell carcinoma. J Urol 171(5):1806–1809

46. Khan MA, Combs CS, Brunt EM, Lowe VJ, Wolverson MK, Solomon H, Collins BT, Di Bisceglie AM (2000) Positron emission tomography scanning in the evaluation of hepatocellular carcinoma. J Hepatol 32(5):792–797

47. Berger KL, Nicholson SA, Dehdashti F, Siegel BA (2000) FDG PET evaluation of mucinous neoplasms: correlation of FDG uptake with histopathologic features. AJR Am J Roentgenol 174(4):1005–1008

48. Jerusalem G, Beguin Y, Najjar F, Hustinx R, Fassotte MF, Rigo P, Fillet G (2001) Positron emission tomography (PET) with 18 F-fluorodeoxyglucose (18 F-FDG) for the staging of low-grade non-Hodgkin's lymphoma (NHL). Ann Oncol 12(6):825–830

49. Tateishi U, Gamez C, Dawood S, Yeung HW, Cristofanilli M, Macapinlac HA (2008) Bone metastases in patients with metastatic breast cancer: morphologic and metabolic monitoring of response to systemic therapy with integrated PET/CT. Radiology 247(1):189–196

50. Huyge V, Garcia C, Vanderstappen A, Alexiou J, Gil T, Flamen P (2009) Progressive osteoblastic bone metastases in breast cancer negative on FDG-PET. Clin Nucl Med 34(7):417–420